

DEVELOPMENT OF DISH-STIRLING CONCENTRATING SOLAR THERMAL-  
ELECTRIC ENERGY CONVERSION SYSTEM

GAN LEONG MING

A thesis submitted in fulfilment of the requirements  
for the award of degree of  
Doctor of Philosophy of Engineering in Automotive

Faculty of Mechanical Engineering  
UNIVERSITI MALAYSIA PAHANG

SEPTEMBER 2012

5/12 P PERPUSTAKAAN UNIVERSITI MALAYSIA PAHANG	
No. Perolehan 087940	No. Panggilan TJ 811 .G36 2012 rs. Thesis
Tarikh 31 OCT 2012	

## ABSTRACT

Sunlight is the world's largest renewable energy source. Using the existing technologies, this energy can provide the needs of all the people on Earth. By increasing the solar-to-electric energy conversion efficiency while maintaining the cost and lifespan of a machine, conventional photovoltaic technology is being progressively challenged by concentrated solar thermal engine technology especially in large scale power plant. For local research, the limitation of technological development between technical potential and practical utilisation of solar energy becomes one of the reasons behind the minimum growth of solar energy field. Owning a local renewable energy conversion system means decrease fossil fuel dependability, secure near to long term power supply chain and hence enhances economic development. In order to develop local expertise with low production cost, full scaled dish-Stirling CST based on DNI solar flux modules were prototyped. The development of the research began with a preliminary assessment on a 2m diameter manual operated ideal paraboloid concentrating dish prototype. Based on the important design parameters and followed by rigorous system design principles, an 8m diameter combined paraboloid-Fresnel concentrating dish with low focus height, low dish height and minimal wind resistance was designed and constructed. Using the hydraulic-electric two-axis solar tracking system, the proposed system was able to move  $0-90^\circ$  in Azimuth axis and  $\pm 180^\circ$  in elevation axis for the full day solar tracking with the consideration of yearly solar path variation. For the thermal-to-mechanical energy conversion, a compact and superior combination of square configuration, four cylinders rhombic drive beta drive mechanism Stirling engine system was integrated with the concentrating dish and tracking mechanism. Throughout the research and development, detailed investigations were conducted to achieve correct operation of the actual prototype. Referring to the 3D model, these studies, including a 3D ray trace analysis on the dish's focal region solar flux concentration pattern, influent of Azimuth angle offset on the thermal receiver performance, air flow simulation on  $\pm 0$  to 28m/s wind load, coefficient of drag comparison and stress distribution due to wind and structural loads. From the computational and operating analysis, the paraboloid-Fresnel dish showed 34.9 to 38.3% of wind load reduction compared with ideal paraboloid design, low  $C_D$  in between 0.077 to 0.76 depends on wind flow direction and rotating angle. Together with structural mass, stress simulation indicated maximum stress of  $320.6\text{MN/m}^2$  and was validated with six components failure. Meanwhile, practical model showed 51% of structural stress reduction after continuous design improvement. Next, focal region temperature readings were recorded under various circumferences, and maximum concentrated temperature of  $357^\circ\text{C}$  had agreed the research hypothesis that specific thermal receiver design can store the solar flux at higher intensity. After several cranking tests, the prototype Stirling engine was unable to start as designed due to scattered solar thermal distribution. Based on Schmidt's analysis, the predicted engine output power was 6.03kW. Considering the total energy consumption for PLC, electric motor, hydraulic system and auxiliary system, the net power output was predicted at 5.759kW. Based on  $1000\text{W/m}^2$  solar DNI, the energy conversion efficiency for 8m diameter concentrating dish was predicted at 11.52%.

## ABSTRAK

Cahaya matahari adalah sumber tenaga boleh diperbaharui yang terbesar di dunia. Dengan menggunakan teknologi yang sedia ada, tenaga ini boleh menyediakan keperluan semua manusia di Bumi. Dengan meningkatkan kecekapan penukaran tenaga solar untuk elektrik sementara mengekalkan kos dan jangka hayat mesin, teknologi photovoltaic konvensional sedang beransur-ansur dicabar oleh tertumpu solar enjin teknologi haba terutama di loji kuasa secara besar-besaran. Bagi penyelidikan tempatan, had pembangunan teknologi antara potensi teknikal dan praktikal penggunaan tenaga solar menjadi salah satu daripada sebab-sebab di sebalik pertumbuhan bertakung bidang tenaga solar. Memiliki sistem penukaran tenaga tempatan yang boleh diperbaharui ertinya mengurangkan pergantungan pada bahan api fosil, kekalkan rantaian bekalan kuasa jangka panjang dan dengan itu meningkatkan pembangunan ekonomi. Dalam usaha untuk membangunkan kepakaran tempatan dengan kos pengeluaran yang rendah, piring/Stirling CST berskala penuh berdasarkan modul fluks solar DNI telah dibangunkan. Pembangunan penyelidikan bermula dengan penilaian awal mengenai piring paraboloid diameter 2m. Berdasarkan parameter reka bentuk yang penting dan diikuti dengan prinsip-prinsip reka bentuk sistem ketat, piring diameter 8m hasil gabungan paraboloid-Fresnel dengan ketinggian tumpuan dan tinggi piring yang rendah, serta rintangan angin minimum telah ditakrifkan dan dibina. Menggunakan hidraulik elektrik dua paksi Penjejakan sistem solar, sistem yang dicadangkan mampu untuk bergerak  $0-90^\circ$  dalam Azimut paksi dan  $\pm 180^\circ$  dalam paksi ketinggian untuk Penjejakan hari solar penuh dengan mengambil kira perubahan laluan solar tahunan. Untuk penukaran tenaga terma kepada mekanikal, kombinasi yang padat dan atasan konfigurasi persegi, empat silinder berbentuk *rhombic drive* enjin *Stirling* jenis beta bersepadu dengan piring pengumpulan cahaya matahari serta mekanisme pegas. Sepanjang penyelidikan dan pembangunan, siasatan terperinci dijalankan untuk mencapai pengendalian yang betul bagi prototaip sebenar. Merujuk kepada model 3D, kajian termasuk ray 3D surih analisis di rantau tumpuan piring kepekatan corak fluks, kesan sudut Azimut diimbangi prestasi penerima haba, udara simulasi aliran dari  $0-28\text{m/s}$  angin beban, pekali perbandingan seret dan agihan tegasan yang disebabkan oleh angin dan beban struktur. Dari analisis pengiraan dan operasi, piring paraboloid-Fresnel menunjukkan 34.9-38.3% pengurangan beban angin berbanding dengan reka bentuk paraboloid yang ideal,  $C_D$  rendah di antara 0.077-0.76 bergantung kepada arah aliran angin dan sudut berputar. Bersama-sama dengan jisim struktur, simulasi tekanan menunjukkan tegasan maksimum  $320.6\text{MN/m}^2$  dan disahkan dengan enam komponen kegagalan. Sementara itu, model praktikal menunjukkan 51% daripada pengurangan tekanan struktur selepas peningkatan reka bentuk yang berterusan. Seterusnya, fokus rantau bacaan suhu dicatatkan di bawah keadaan pelbagai, dan suhu maksimum pekat  $357^\circ\text{C}$  telah bersetuju hipotesis penyelidikan bahawa penerima reka bentuk haba tertentu boleh menyimpan fluks solar pada intensiti yang lebih tinggi. Selepas beberapa ujian cuba hidupan enjin, prototaip Stirling enjin tidak dapat beroperasi seperti yang direka bentuk kerana rata berselerak panas matahari. Berdasarkan analisis Schmidt, kuasa enjin yang diramalkan adalah 6.03kW. Dengan mengambil kira jumlah penggunaan tenaga untuk PLC, motor elektrik, sistem hidraulik dan sistem bantu, kuasa keluaran bersih diramalkan pada 5.759kW. Berdasarkan  $1000\text{W/m}^2$  solar DNI, kecekapan penukaran tenaga bagi piring diameter 8m telah diramalkan pada 11.52%.

## TABLE OF CONTENTS

		<b>Page</b>
<b>SUPERVISOR'S DECLARATION</b>		ii
<b>CANDIDATE'S DECLARATION</b>		iii
<b>DEDICATION</b>		iv
<b>ACKNOWLEDGEMENTS</b>		v
<b>ABSTACT</b>		vi
<b>ABSTRAK</b>		vii
<b>TABLE OF CONTENTS</b>		viii
<b>LIST OF TABLES</b>		xii
<b>LIST OF FIGURES</b>		xiii
<b>LIST OF ABBREVIATIONS</b>		xix
<b>CHAPTER 1</b>	<b>INTRODUCTION</b>	1
1.1	Background Study on Solar Power	1
1.2	Problem Statement	3
1.3	Objectives	4
1.4	Work Scope	5
1.5	Hypothesis	5
1.6	Flow Chart	6
1.7	Schedule of Work	7
<b>CHAPTER 2</b>	<b>LITERATURE REVIEW</b>	8
2.1	Sustainability and Energy from Nature	8
2.2	Energy Transition to Renewable Resources	9
2.3	Solar Irradiation Distribution and Potential	11
2.4	Worldwide and Local Renewable Energy on Demand	13
2.5	Concentrating Solar Power	15

	2.5.1	Concentrating Solar Thermal Energy	18
	2.5.2	Comparison of Various CST Systems	20
	2.5.3	Development of Concentrating Dish-Stirling	24
2.6		Development of Stirling Engine	28
	2.6.1	Types of Stirling Engine	29
	2.6.2	Stirling Engine for Solar Thermal Power	30
	2.6.3	Ideal Stirling Cycle	31
	2.6.4	Effect of Phase Angle and Practical Losses	36
	2.6.5	Attractions and Drawbacks	40
	2.6.6	Working Fluid Properties	42
	2.6.7	Drive Mechanism	45
2.7		Solar Concentrating System	47
	2.7.1	Solar Flux Collector	47
	2.7.2	Solar Thermal Receiver	50
	2.7.3	Ray Trace of Focal Point Thermal Distribution	52
	2.7.4	Reflector and Receiver Material Properties	60
	2.7.5	Mathematical Analysis	64
2.8		Energy Storage and Hybridisation	69
2.9		Solar Tracking	72
<b>CHAPTER 3 METHODOLOGY</b>			<b>75</b>
3.1		Solar Irradiation Concentrator	76
	3.1.1	Feasibility Assessment of 2m Diameter Concentrating Dish Technology	76
	3.1.2	Conceptual Design of 8m Diameter Solar Flux Concentrating Dish	81
	3.1.3	Solar Concentrating Dish Working Model Development	89
3.2		Two-axis Intermediate Solar Tracking System	96
	3.2.1	System Operation Design	97
	3.2.2	Working Model Development	100
3.3		Solar Thermal Receiver	107
3.4		Square Rhombic Drive Multi Cylinders Stirling Engine Development	112
3.5		Overall System Integration	123
3.6		Dish-Stirling Monitoring and Data Acquisition System	125
3.7		Computational Analysis of Dish-Stirling System	128

	3.7.1	Air Flow Analysis on Concentrating Dish	129
	3.7.2	Structural Analysis on Solar Concentrator and Solar Tracking Mechanism	130
	3.7.3	3D Ray Trace Analysis on Concentrating Dish	132
	3.7.4	Thermodynamic Analysis on Rhombic Drive Beta Stirling Engine	135
<b>CHAPTER 4</b>		<b>RESULTS AND DISCUSSIONS</b>	<b>138</b>
4.1		Paraboloid-Fresnel Concentrating Dish Design Parameters	138
4.2		Solar Irradiation Distribution on Focal Region	141
	4.2.1	DNI Distribution and Boundary Setting	142
	4.2.2	Solar Points Distribution	144
	4.2.3	Feasibility on Receiver/Secondary Reflector Design	147
4.3		Dish-Stirling Working Model Development	151
	4.3.1	Concentrating Dish	151
	4.3.2	Two-axis Solar Tracking System	155
	4.3.3	Solar Thermal Receiver and Secondary Reflector	157
	4.3.4	Square Rhombic Drive Beta Stirling Engine	161
	4.3.5	Dish-Stirling System Integration and On-Site Installation	169
4.4		Air Flow Simulation on Concentrating Dish	171
	4.4.1	Boundary Condition Setting	171
	4.4.2	Air Flow Distribution	173
	4.4.3	Force Effect for Focus Height and Dish Height Variation	177
	4.4.4	Wind Drag Analysis	180
	4.4.5	Resultant Force on Hydraulic System	181
4.5		Structural Load Analysis	186
	4.5.1	Boundary Condition Setting	186
	4.5.2	Case 1 : Failure Analysis on Original Prototype	189
	4.5.3	Case 2 : Design Refinement for Second Prototype	195
4.6		Working Model Analysis	202
	4.6.1	Solar Receiver and Secondary Reflector Analysis	202
	4.6.2	Concentrating Dish Operation	211
	4.6.3	Thermal Engine Operational Analysis	214
	4.6.4	System Energy Consumption and Efficiency	231

<b>CHAPTER 5</b>	<b>CONCLUSION AND RECOMMENDATION</b>	<b>238</b>
5.1	Research Summary	238
5.2	Conclusions	239
5.3	Recommendations	241
	<b>REFERENCES</b>	<b>243</b>
	<b>APPENDICES</b>	<b>251</b>
A	Research Gantt Chart	252
B	Development of 2m Diameter Paraboloid Concentrating Dish	253
C	Optimisation Calculation on Reflecting Angle and Dish Height Based on Paraboloid-Fresnel Principle	256
D	Thermocouple Dimension and Installation	259
E	Direct Normal Irradiation Reading	262
F	Solar Flux Distribution	263
G	Dish-Stirling System Development	273
H	Air Flow Simulation	284
I	Static and Wind Load Analysis	288
J	Schmidt Cycle Analysis	295

## LIST OF TABLES

<b>Table No.</b>	<b>Title</b>	<b>Page</b>
2.1	Comparison between various CST system	23
2.2	Development of dish-Stirling CST and technical viability of this technology for generating power	25
2.3	Parasitic losses in Stirling engine	37
2.4	Effect of regenerator on Stirling engine performance referred to GPU-3 model	39
2.5	Working fluid properties comparison at 1 atm, 300K	43
2.6	Specular reflectance values for different reflector materials	62
3.1	Preliminary assessment on paraboloid concentrating dish with two-axis control mechanisms	80
3.2	Comparison of different reflecting shape	83
3.3	Various operation modes for concentrating dish	100
3.4	Dimension definitions for rhombic drive mechanism	114
3.5	Static stress analysis solar concentrating system	134
4.1	Boundary condition setting on 3D sun ray tracing and focal region distribution	143
4.2	Concentrating dish model dimension for air flow simulation	173
4.3	Air Flow result of Ideal Paraboloid I Design	174
4.4	Air Flow result of Ideal Paraboloid II Design	175
4.5	Air Flow result of Paraboloid-Fresnel Design	176
4.6	TDC and BDC for 44° phase angle rhombic drive system	216
4.7	Engine volumetric displacement at TDC and BDC	217
4.8	Engine dynamic test conditions	218
4.9	Summary of single cylinder thermodynamic parameters	228
4.10	Single and four cylinders configuration power output at 2000rpm	230
4.11	Total energy consumption analysis	237



## LIST OF FIGURES

Figure No.	Title	Page
1.1	Annual solar irradiance on Earth	2
2.1	Definition of sustainability	8
2.2	Energy conversion scheme	9
2.3	Solar irradiation versus established global energy resources	12
2.4	Solar irradiation and yearly variations of the solar constant at outer atmosphere	12
2.5	Sunbelt countries	13
2.6	Estimate of the number of days where DNI falls below 3000kWh/m <sup>2</sup>	16
2.7	Simplified analytic CSP solar output profile by time of the day	17
2.8	Various concentrating solar power technologies	18
2.9	Performance of different solar systems	19
2.10	Dish engine system block diagram	22
2.11	Three basic mechanical configurations for Stirling engine	29
2.12	Stirling cycle	32
2.13	Ideal Stirling engine thermodynamic cycle	33
2.14	PV diagram for phase angle range between 0 to 175°	36
2.15	Performance of different regenerator matrix porosity on various phase angle	40
2.16	Variation of brake power with heat source temperature	42
2.17	Possible concentrating collector configurations a. tubular absorbers with diffuse back reflector, b. tubular absorbers with specular cusp reflectors, c. plane receiver with plane reflectors, d. parabolic concentrator, e. Fresnel reflector, f. Linear Fresnel reflector with central receiver	48
2.18	Schematic diagram of relationship between Earth and Sun	53
2.19	The thermal efficiency of a receiver $\eta_{th}$ as a function of the fluid temperature $T_F$ and concentration factor C based on 800 W/m <sup>2</sup> solar irradiation	54
2.20	The laws of reflection and refraction	55
2.21	Modelling and sampled ray display generated from the ray tracing results	56
2.22	Comparison of the radiative flux distribution between the real concentrator and the ideal paraboloidal concentrator for the real sun case	57
2.23	Effect of the receiver position on the radiation flux distribution and radiation collecting efficiency	58
2.24	Variations in temperature for various radii	59

2.25	Types of reflection from surfaces	61
2.26	Solar Flux Map in the focal plane normalized to $1000\text{W}/\text{m}^2$	64
2.27	Schematic diagram for parabolic dish concentrating system	65
2.28	Combination of storage and hybridisation in a solar plant	70
2.29	Concept of Hydrogen internal combustion Stirling engine	72
2.30	Definition of solar altitude and azimuth angles	73
2.31	Various two-axis solar tracking system	74
3.1	Solar thermal dish-Stirling development block diagram	75
3.2	2m diameter concentrating dish with manual tracking system	77
3.3	Proposed operation for solar tracking	78
3.4	Design detail of 2m diameter concentrating dish	79
3.5	Development of working prototype model	79
3.6	Variation of total wind force on the collector for various collector orientations and wind velocities	85
3.7	Mathematical definition of Paraboloid-Fresnel Design	86
3.8	Concentrating dish segment division	90
3.9	3D design of centre block	91
3.10	3D design of dish supporting structure	92
3.11	Design of poly-frame for different dish segments	93
3.12	Design of reflecting angle adjustor	93
3.13	Design of reflecting surface	94
3.14	Sub-assembly of solar concentrating dish – load supporting structure	95
3.15	Sub-assembly of solar concentrating dish – segment assembly with reflecting mirrors	95
3.16	Assembly view of the solar concentrating dish design	96
3.17	Typical Malaysia's annual variation of sun path diagram	97
3.18	Solar tracking system – Integration between mechanism and control units	98
3.19	Solar, wind and rain sensor	99
3.20	Design of azimuth angle control unit	101
3.21	Working principle of the azimuth angle control unit	102
3.22	Design of elevation angle control unit and dish supporting structure	103
3.23	Integration of two-axis solar tracking mechanism	104
3.24	Alignment of the concentrator and solar sensor using a compass	105
3.25	Full assembly view of solar concentrating dish	106
3.26	Basic operation mode of solar tracking system based on solar time	106
3.27	Conceptual design of solar concentrator focal region	107
3.28	Design of solar thermal receiver	109
3.29	Design of solar thermal absorber coil	110

3.30	Design of secondary reflector model 1	111
3.31	Design of secondary reflector model 2	112
3.32	2D sketch of a Beta Stirling engine with rhombic drive mechanism	113
3.33	3D design of identical set of Beta Stirling engine with rhombic drive mechanism	115
3.34	Power multiplication module design	116
3.35	3D illustration of square rhombic drive Stirling engine assembly	117
3.36	Displacer and power cylinder design and assembly	118
3.37	Regenerator material selection	119
3.38	Complete design of square rhombic drive beta Stirling engine system	120
3.39	Water cooling system operation	121
3.40	Lubricating system operation	122
3.41	Engine starting motor and power output drive mechanism	123
3.42	Completed assembly of engine, receiver and power generator	124
3.43	Full integration of dish-Stirling concentrating solar thermal system	125
3.44	Dish-Stirling monitoring System	126
3.45	Dish-Stirling monitoring sensors	126
3.46	Thermocouple variation for different application	127
3.47	DAQ unit and calibration procedures	128
3.48	Modelling of simplified 3D cone mirror arrays concentrator	129
3.49	Solar flux meter	130
3.50	Annual frequency distribution of wind speeds in Mersing	131
3.51	Daily mean wind speed for Subang Malaysia throughout a typical year	131
3.52	Weight distribution for solar concentrator with and without engine assembly	133
3.53	Engine efficiencies as a function of phase angle for various losses	136
4.1	Intersection of $Y_a$ and $Y_b$ for the reflecting angle definitions	139
4.2	Optimised reflecting angle for various layer of reflecting mirrors	140
4.3	Corresponding mirror height, $Y_s$ referred to each layer reflecting angle	140
4.4	Comparison between Paraboloid-Fresnel and ideal parabolic dish	141
4.5	DNI result from 8:00am to 6:00pm for measured days	142
4.6	Modelling of paraboloid-Fresnel solar concentrators	143
4.7	Solar flux input and reflection to focus plane	144
4.8	Solar flux distribution on 2m height focus point range 200-1200W/m <sup>2</sup> (0° azimuth offset)	145

4.9	Focal region shape and size variation in different azimuth offset angle ( $H_f=2000\text{mm}$ )	146
4.10	Focal region area distribution for different azimuth angle offset (referred to various focus height)	147
4.11	Relationship between receiver assembly and focus plane	148
4.12	Percentage of overlap between external receiver and focal region for various focus height	149
4.13	Percentage of overlap between cavity receiver model 1 and focal region for various focus height	150
4.14	Percentage of overlap between cavity receiver model 2 and focal region for various focus height	150
4.15	Fabrication of centre block	152
4.16	Fabrication of dish supporting structure	152
4.17	Fabrication of poly-frame structure for segment A, B, C and D	153
4.18	Completed poly-frame structure and reflecting mirrors	154
4.19	Assembly of 8m paraboloid-Fresnel concentrating dish	155
4.20	Elevation control mechanism	156
4.21	Azimuth control mechanism	156
4.22	Load supporting structures	156
4.23	Assembly of two-axis solar tracking system	157
4.24	Assembly of solar thermal receiver	158
4.25	Integration of external receiver	159
4.26	Integration of secondary reflector model 1	160
4.27	Integration of secondary reflector model 2	160
4.28	Stirling engine interior components	161
4.29	Stirling engine exterior engine blocks	162
4.30	Assembly of power cylinder and upper yoke	163
4.31	Assembly of engine main moving components	163
4.32	Assembly of power multiplication module	164
4.33	Assembly of power cylinders, water jacket and regenerator	165
4.34	Assembly of power cylinders, water jacket and regenerator	166
4.35	Completion of multi cylinders square rhombic drive beta engine	167
4.36	Installation of auxiliary components	168
4.37	Completed integration between engine, receiver and absorber	169
4.38	Sub integration of dish-Stirling system	170
4.39	Integration of dish-Stirling system	171
4.40	Air flow computational simulation boundary condition setting	172
4.41	Wind load on 8m diameter ideal Paraboloid I vs wind speed for 0-90° dish rotation	177
4.42	Wind load on 8m diameter ideal Paraboloid II vs wind speed for 0-90° dish rotation	178
4.43	Wind load on 8m diameter Paraboloid-Fresnel dish vs	179

	wind speed for 0-90° dish rotation	
4.44	Coefficient of drag ( $C_D$ ) vs dish rotating angle for different case study	180
4.45	Structural load distribution of hydraulic system for zero wind load	182
4.46	Structural load distribution on hydraulic cylinder for zero wind load	182
4.47	Total load on hydraulic system vs dish rotating angle	184
4.48	Total load on hydraulic cylinder vs dish rotating angle	185
4.49	Static load analysis boundary condition setting	187
4.50	Input load setting for static load analysis	188
4.51	Von Mises stress distribution for dish structure (zero wind load without engine)	189
4.52	Von Mises stress distribution for dish structure (zero wind load with engine)	190
4.53	Critical component minimum Factor of safety comparison	191
4.54	Factor of Safety for dish structure	192
4.55	Structural failure on proposed dish-Stirling system	193
4.56	Bearing failure validation	194
4.57	Shaft failure due to overloading	195
4.58	Structural displacement plot	195
4.59	Development of second model	196
4.60	Stress distribution plot for dish with engine system under maximum wind load condition	197
4.61	FOS distribution plot for dish with engine system under maximum wind load condition	198
4.62	Maximum stress distribution under different circumferences	199
4.63	Maximum strain distribution under different circumferences	200
4.64	Maximum displacement plot under different circumferences	201
4.65	Minimum FOS plot under different circumferences	201
4.66	Second model working prototype	202
4.67	Temperature distribution for external receiver on 14 Oct 2011	204
4.68	Temperature distribution for secondary reflector model I without lenses on 28 Oct 2011	205
4.69	Temperature distribution for secondary reflector model 1 with lenses on 31 Oct 2011	206
4.70	Temperature distribution for secondary reflector model 2 on 01 Nov 2011	208
4.71	Deficiency due to mirror defeats	209
4.72	Temperature distribution for secondary reflector model II after mirror tuning on 10 Nov 2011	210
4.73	On site solar variation from 10am to 7pm	211
4.74	Definition of single acting and double acting	212
4.75	Solar tracking system operation	213

4.76	Scopes of engine operational analysis	214
4.77	Engine components reciprocating displacement plot for 44° phase angle	215
4.78	Periodic volumetric displacement (cylinder 1) for proposed engine model	217
4.79	Temperature result under condition A	219
4.80	Temperature result under condition B	220
4.81	Temperature result under condition C	221
4.82	Temperature result under condition D	222
4.83	Temperature result under condition E	223
4.84	Inertial constraint due to original setting	224
4.85	Refined engine timing setting	225
4.86	Temperature result under condition F	226
4.87	P-V diagram for different phase angle setting	227
4.88	Multi cylinders total effective volume variation for a complete engine cycle	228
4.89	Multi cylinders pressure distribution for a complete engine cycle	229
4.90	Power output prediction under various engine speed calculation	230
4.91	Power output variation under various engine speed calculation	231
4.92	Hydraulic system voltage and current distribution	232
4.93	Electric motor voltage and current distribution	233
4.94	Two-axis control system voltage and current distribution	234
4.95	Auxiliary system voltage and current distribution	235
4.96	Hydraulic system and electric motor power consumption	236
4.97	Overall system power consumption	237

## LIST OF ABBREVIATIONS

### Capital Letters

$A_a$	Reflector area
$A_r$	Receiver area
$A_w$	Cavity internal area of receiver
$A_c$	Entrance aperture area of receiver
BDC	Bottom Dead Centre
CSP	Concentrating solar power
CST	Concentrating solar thermal
$C_D$	Coefficient of drag
$C_p$	Specific heat capacity at constant pressure
$C_v$	Specific heat capacity at constant volume
CR	Geometric concentration ratio
$CR_o$	concentration ratio
DNI	Direct Normal Irradiation
$E$	Total emissive power
$E_b$	Total emissive power of a blackbody
F	Force
FOS	Factor of safety
$H_f$	Focus height
$H_d$	Dish height
$I_a$	Reflector solar flux
$I_r$	Receiver solar flux
$L_0$	Distance between the Sun and the Earth = $1.496 \times 10^{11}$ m
M	Moment
Mtoe	Million Tonnes of Oil Equivalent
$P$	Working gas pressure
PLC	Programmable logic control
$P_{min}$	Minimum working pressure
$P_{max}$	Maximum working pressure

$P_{mean}$	Mean working pressure
PV	Photovoltaic
$Q$	Heat transfer
$Q_H$	Heat source or sink per unit volume
$Q_s$	Solar energy incident on the concentrating dish
$Q_r$	Radiant solar energy falling on the receiver
$Q_l$	Heat losses from the receiver to the surroundings
$Q_u$	Useful energy collected
$Q_{lo}$	Optical loss from the collector
$Q_{lk}$	Conductive heat loss from receiver
$Q_{lc}$	Convective heat loss through the receiver aperture
$Q_{tr}$	Radiative heat loss through the receiver aperture the focusing device
$R$	Gas constant
$R_{s\ n}$	Dish front radius for mirror in section n
$R_{c\ n}$	Dish centre radius for mirror in section n
$R_{e\ n}$	Dish end radius for mirror in section n
$S_i$	Mass distributed external force per unit mass
$T$	Working gas temperature
TDC	Top Dead Centre
TW	Terawatts
TWh	Terawatts hour
$T_{min}$	Working fluid minimum temperature
$T_{max}$	Working fluid maximum temperature
$T_w$	Average operating wall temperature in the cavity
$T_a$	Ambient temperature
$V$	Working gas volume
$W$	Work done
$W_c$	Compression work done
$W_e$	Expansion work done
$W_{net}$	Net-work done



**Small Letters**

$d_r$	Concentrating dish diameter
$d_f$	Focus area diameter
$d_{sun}$	Diameter of the Sun= $1.392 \times 10^9$ m
$d_{earth}$	Diameter of the Earth= $d_{sun}/10^9$
$h$	Thermal enthalpy
$h_c$	Convective heat transfer coefficient
$l_n$	Reflected sun ray length
$l_m$	Faceted mirror length
$m$	Mass of working gas
$n$	Mirror section
$pf$	Paraboloid focus point
$q_i$	Diffusive heat flux
$r_i$	Sun ray incoming vector
$r_t$	Sun ray refraction vector
rpm	revolution per minute
$r_v$	Compression ratio
$s$	Entropy
$x$	X-axis coordinate
$y$	Y-axis coordinate
$y_{s n}$	Front height for mirror in section n
$y_{c n}$	Centre height for mirror in section n
$y_{e n}$	End height for mirror in section n
$y'_{s n}$	Front height for ideal parabolic in section n
$y'_{c n}$	Centre height for ideal parabolic in section n
$y'_{e n}$	End height for ideal parabolic in section n

**Greek Symbols**

$\alpha$	Absorptivity
$\alpha_t$	Thermal diffusivity
$\gamma$	Ratio of the energy intercepted by the receiver to the energy reflected by
$\varepsilon$	Emissivity
$\varepsilon_c$	Cavity surface emittance

$\epsilon_{eff}$	Effective infrared emittance of cavity
$\eta_t$	Thermal efficiency
$\eta_{plant}$	Plant efficiency
$\eta_{col}$	Solar collector efficiency
$\eta_{ref}$	Reflector efficiency
$\eta_{eng}$	Engine efficiency
$\eta_o$	Optical efficiency
$n_i$	Sun ray incoming ratio
$n_t$	Sun ray refraction ratio
$\theta$	Solar incidence angle
$\theta_n$	Faceted mirror angle
$\theta_i$	Sun ray incoming angle
$\theta_r$	Sun ray reflecting angle
$\theta_t$	Sun ray refraction angle
$\theta_a$	Sun's radiation cone maximum half angle
$\theta_\alpha$	Solar altitude angle
$\theta_\beta$	Solar azimuth angle
$\theta_\delta$	X-axis angle
$\theta_L$	Y-axis angle
$\theta_H$	Z-axis angle
$\theta_{rim}$	Half angle subtended by the arc of the parabola
$k$	Thermal diffusivity
$\lambda$	Factor of un-shading
$\sigma$	Stress
$\sigma_{vonMises}$	Von mises stress
$\sigma_{limit}$	Maximum stress
$\sigma_S$	Stefan-Boltzmann constant, $5.67 \times 10^{-8} \text{ W}/(\text{m}^2\text{K}^4)$
$\rho$	Fluid density
$\rho_r$	Reflectivity
$\rho_{gas}$	Working gas density
$\tau$	Transmissivity
$\tau_{ik}$	Viscous shear stress tensor

$\tau_t$	Temperature ratio
$\Omega$	Angular velocity.

## CHAPTER 1

### INTRODUCTION

#### 1.1 Background Study on Solar Power

Due to environmental issues as well as increasing demand for renewable resource, the conversion of solar power into useful energy is receiving more and more attention in recent years. Sunlight is the world's largest energy source. The amount that can be readily accessed with existing technology greatly exceeds the world's primary energy consumption. Furthermore, sunlight is free, clean, renewable and technically exploitable in most part of the inhabited earth (Angkee and Chana, 2011).

Taking the Sun as the spectrum of a blackbody at 5800K, the amount of solar energy falling on a surface per unit area and per unit time is illustrated in Figure 1.1. Currently, the Sun radiates energy at  $3.9 \times 10^{26} \text{W}$  or  $64 \times 10^6 \text{W/m}^2$  but energy received by the Earth and its atmosphere is  $1368 \text{W/m}^2$  or  $1.7 \times 10^{17} \text{W}$  of radiation yearly from the sun. This value varies in  $\pm 1.7\%$  due to changes in the Earth-Sun distance (Salsabila, Ab Kadir and Suhaidi, 2011). Assuming that the world population is 10 billion with a total power need per person of 10kW would require about  $10^{11} \text{kW}$  of energy (Goswami, Frank and Jan, 2000). This is equal to 1000km x 1000km solar powered land area plotted in the middle of the Atlantic Ocean (Anton and Christian, 2009). Apparently, solar irradiance on only 1% of the earth's surface with 10% efficiency useful energy conversion could provide the needs of all the people on Earth (Goswami, Frank and Jan, 2000).

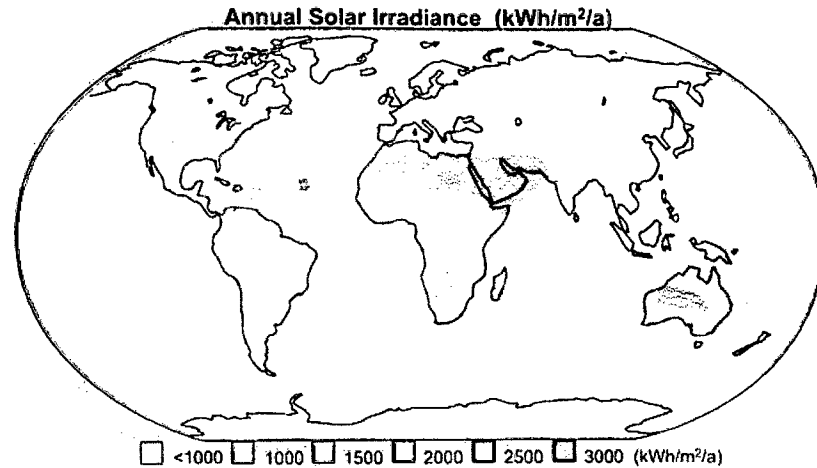


**Figure 1.1** : Annual solar irradiance on Earth

Source : Anton and Christian (2009)

A tropical country such as Malaysia is generally hot all year-round and experiences its rainy season during the end of the year. Within an average of 12 hours of sunshine daily, the average solar energy received is between 1400 and 1900kWh/m<sup>2</sup> annually. The maximum radiation is received during a sunny day, where 90% of the extraterrestrial radiation becomes direct radiation while the rests are being deflected as diffuse radiation, while conversely, on a cloudy day, nearly all the solar radiation is diffused (Salsabila, Ab Kadir and Suhaidi, 2011). The weather condition in Malaysia is suitable for solar power implementation. This is because the weather condition is almost predictable and the availability of about 6h of direct sunlight with irradiation of between 800W/m<sup>2</sup> and 1000W/m<sup>2</sup> (Nowshad, Chin and Kamaruzzaman, 2009).

Today, two technologies are being actively developed to transform solar irradiation into electricity. One technology is photovoltaic or solar voltaic which uses photovoltaic materials to convert solar radiation directly into electricity. The other technology is solar thermal power or concentrating solar power converts the solar radiation into heat and then electricity through various thermodynamic cycles. For photovoltaic cells, efficiency up to 18% are reported while the efficiency of heat engine conversion systems can be as high as 33% depending on the quality of the technology used (Karabulut, Yucesu and Cinar, 2006). Restricted by the capital cost of solar panels

and other issues, the photovoltaic technology is being increasingly challenged by solar thermal power technology. In recent years, some practical solar thermal power plants have been installed in countries such as the US, Europe, India and China (Wu, Xiao, Cao and Li, 2010).

## 1.2 Problem Statement

Compared with the heavily subsidised fossil fuel, renewable energy such as solar power often labeled as expensive and will never be price-competitive. In addition, solar technology has been always stereotyped as not technically feasible for electricity generation due to the high cost. Although solar power has an enormous potential to reduce the global emissions of greenhouse gasses, the current use of this energy resource represents less than 1% of the total electricity production from renewable sources (Goswami, Frank and Jan, 2000). Particularly in Malaysia, the present initiatives and efforts are lower than the country's actual potential. Currently, the solar status in Malaysia is 1MW, but its estimated potential can reach more than 6500MW (Salsabila, Ab Kadir and Suhaidi, 2011). The limitation of technological development between technical potential and practical utilisation of solar energy becomes one of the reasons behind the minimum growth of solar-energy field.

The total solar energy reaching the earth is made up of two parts; energy from direct irradiation and energy from diffused irradiation. Although power-plants can use direct and diffuse solar energy, most of the man-made solar-electric conversion system can convert only direct energy efficiently (Goswami, Frank and Jan, 2000). With the solar concentration system, high intensity solar thermal engine operation is much more efficient than the diffuse solar technology.

In the recent development, one of the most viable technologies is the concentrating solar thermal (CST) which is able to convert solar electric for both distributed and remote area applications. However, each energy conversion has efficiency, cost and an environmental footprint depending on the worthiness of the process. From a scientific and technical viewpoint, the development of new technologies with higher conversion efficiencies and low production costs become the

key requirement for enabling the deployment of solar energy at a large scale (Goswami, Frank and Jan, 2000).

For the dish-Stirling CST technology as instance, it has good potential in power modulation and possess high concentration ratio. However, the solar-to-electric efficiency varies largely depending upon the solar flux density, concentration factor, the temperature of the thermal intermediary and the thermal cycle efficiency for the production of mechanical work and electricity. In order to maximise the solar fraction, intense search for effective and economic methods to capture, store and convert solar energy into useful energy should not be neglected (Mekhilef, Saidur and Safari, 2011).

In order to do that, one of the crucial steps is the introduction of specific solar thermal-electric energy conversion technology. In the case of dish-Stirling system, the technology development includes concentrator, receiver, absorber, thermodynamic cycle and tracking system. The technology must be further developed and proven to be technically and economically feasible with the consideration of environmental impact such as material degradation and climate constraints.

### **1.3 Objectives**

Research objectives for the development of solar thermal energy conversion system are listed as follows:

- i. To prototype 8m diameter innovative solar thermal concentrating dish with two-axis solar tracking system
- ii. To develop compact multi cylinders solar Stirling engine with thermal receiver unit for concentrated solar flux operation
- iii. To analyse the operation feasibility of integrated full scale solar dish-Stirling prototype model.

## 1.4 Work Scope

The work scope is specified as follows:

- i. Development of solar thermal concentrator based on combined paraboloid-Fresnel principle
- ii. Development of azimuth-elevation control unit, load supporting structures and direct normal irradiation tracking system
- iii. Development of a square rhombic drive Stirling engine incorporated with the solar-thermal receiver
- iv. Integration of working prototype dish-Stirling system
- v. Installation of data acquisition and monitoring sensors
- vi. Dish-Stirling working model operational analysis.

## 1.5 Hypothesis

Large concentrating dish development based on innovated paraboloid-Fresnel concept could minimise wind and rain load which indeed applicable for modular or distributed tropical application. Consistent solar tracking system could be developed using PLC principle and accumulation of high intensity solar direct normal irradiation. Consequently, it could increase the temperature of thermal flux in the specific receiver-absorber to drive the four-cylinder square type rhombic drive beta Stirling engine. For the solar power conversion, solar thermal is an alternate solution instead of the photo-chemical process.